Ultrahigh-Resolution Electron Energy Loss Spectroscopy via Digital Signal Processing Techniques

Youqi Wang and W. Henry Weinberg

Department of Chemical Engineering, University of California, Santa Barbara, California 93106-5080

The methodology underlying a novel spectral analysis is presented for inelastic electron scattering from solids. Implementation of the method involves Fourier transformation of the measured spectrum and deconvolution in the Fourier domain, spectral estimation using the maximum entropy method, and line-shape analysis using Gaussian and Lorentzian functions, all performed in the Fourier domain. The utility of the method is demonstrated for the case of vibrationally inelastic electron scattering from CO adsorbed on Ru(001).

PACS numbers: 61.16.–d, 06.50.Dc, 68.45.Da, 68.45.Kg

Since the pioneering work of Propst and Piper [1], inelastic electron scattering from surfaces, also known as electron energy loss spectroscopy (EELS), has become one of the most important tools in the study of the vibrational properties of solid surfaces [2,3]. Applications of the technique range from elucidating vibrational structures of chemically and physically adsorbed overlayers to mapping dispersion relations of surface phonons. Some of the advantages of EELS compared, for example, to an optical spectroscopy such as infrared reflection-absorption spectroscopy (IRAS) [4,5] include the following: (1) higher sensitivity, (2) wider dynamic detection range, and (3) selection rules that permit observation of optically forbidden modes (those oriented parallel to the surface). The major disadvantage of EELS has been its relatively poor resolution compared to optical spectroscopies. Much progress has been made in the past 25 years in the design and construction of electron beam monochromators and energy analyzers and their associated electronics [6], and recently Ibach's group have published spectra with a resolution of 1 meV (FWHM of the elastically scattered peak) [7]. It remains, however, rather difficult to obtain energy loss spectra with a FWHM below 4–5 meV, and "high-resolution" EELS is generally applied to those spectra with a FWHM below 10 meV.

Despite these remarkable improvements in the "hardware" associated with EELS, the development of "software" to process the data is still in its infancy. In studies of metal oxide surfaces, deconvolution techniques have been implemented to suppress surface phonon modes [8,9]. Because of difficulties inherent in deconvolution schemes [10,11], this technique improves neither the spectral resolution nor the signal-to-noise ratio (SNR). Curve-fitting techniques have been combined with measurements of the instrument response function (the FWHM of the elastically scattered peak in this case) with the goal of obtaining the true linewidth of surface vibrational modes [12,13]. This procedure is of limited use, however, since *a priori* knowledge of the number of peaks in a spectrum and their shapes is required, a problem that is common to all curve-fitting schemes [14].

In this Letter, we describe a novel spectral analysis method which is capable of eliminating all broadening due to the instrument response function. A complete discussion of our procedure, including all details and sensitivity analyses, will be published elsewhere [15]. This procedure allows, for the first time, a determination of the natural line shapes of the physical or chemical system being investigated. In addition to this improvement in resolution, the spectral SNR is also increased by orders of magnitude. Although we apply our method here to the problem of vibrational EELS, the algorithm is quite general and can be used in connection with any spectroscopy for which the instrument response function can be obtained accurately from either experiment or theory.

A measured EEL spectrum can be expressed mathematically as [15]

$$s(E) = i(E) * c(E) + n(E) , \qquad (1)$$

where $s(E)$ is the measured spectrum as a function of loss energy E, $i(E)$ is the instrument response function [16], $c(E)$ is the transfer function of the chemical system (a scattering function), $n(E)$ takes into account noise, and the symbol $*$ denotes a convolution operation. Note that

$$c(E) = \delta(E) + c_i(E) , \qquad (2)$$

where $\delta(E)$ and $c_i(E)$ account for elastic and inelastic scattering, respectively. Substituting Eq. (2) into Eq. (1) gives

$$s(E) = i(E) + i(E) * c_i(E) + n(E) . \qquad (3)$$

It is clear from Eq. (3) that the measured elastic peak is an accurate representation of the instrument response function. Since the elastic peak intensity is typically 2 to 3 orders of magnitude greater than those of the inelastic peaks [2,3], $i(E)$ can be determined experimentally with high accuracy. Taking the Fourier transform of Eq. (1) and rearranging terms gives

$$\frac{S(\tau)}{I(\tau)} = C(\tau) + \frac{N(\tau)}{I(\tau)} , \tag{4}$$

where capital letters denote functions in the Fourier domain, τ. Notice that the left-hand side of Eq. (4) may be constructed from measured spectral data, and the first term on the right-hand side describes fully the scattering function with no interference from the instrument response function, i.e., the latter has been deconvoluted from the former.

The maximum entropy method (MEM) [17–19] may be used for spectral estimation. In this connection we define

$$S'(\tau) \equiv \frac{S(\tau)}{I(\tau)} \quad \text{and} \quad N'(\tau) \equiv \frac{N(\tau)}{I(\tau)} , \tag{5}$$

which implies that $S'(\tau) = S(\tau) + N'(\tau)$. We next define a "cutoff" point, $\tau_{\max}$, in the Fourier domain such that

$$\left| \frac{S'(\tau)}{N'(\tau)} \right| \equiv \left| \frac{S(\tau)}{N(\tau)} \right| \gg 1, \quad |\tau| \leq \tau_{\max} , \tag{6}$$

and we solve

$$\hat{R}\boldsymbol{\alpha} = q\boldsymbol{\beta} , \tag{7}$$

where $\boldsymbol{\alpha} = (1, \alpha_1, \alpha_2, \ldots)^T$, $\boldsymbol{\beta} = (1, 0, 0, \ldots)^T$, and $R_{ij} = \langle S'(\tau_n) S'(\tau_{n+i-j}) \rangle$, $i, j = 1, 2, \ldots, m$. Here, $\hat{R}$ is the autocorrelation matrix, $\boldsymbol{\alpha}$ is the autoregression coefficient vector (to be determined), q is a scaling factor (also to be determined), $\boldsymbol{\beta}$ is a unit vector, and m is the total number of deconvoluted spectral data points in the Fourier domain that satisfy Eq. (6). The scattering function, $c(E)$, can then be estimated by

$$c(E) \approx \frac{|q|}{\left| 1 + \sum_{\ell=1}^{m-1} \alpha_\ell e^{iE\tau_\ell} \right|} . \tag{8}$$

The approximation in Eq. (8) is due to the truncation of $S'(\tau)$. By taking the second derivative of Eq. (8), the following information can be obtained: (1) the total number of spectral peaks, M; (2) the frequency of each peak, E_k ($k = 1, 2, \ldots, M$); and (3) an approximate estimate of the intensities and linewidths of each peak. Note that the total number of peaks may be inflated both by peaks resulting from a nonflat baseline in the original spectrum and by peaks resulting from excessive noise or extremely low count rates in that part of the spectrum where they appear. The former are characterized by very broad peak widths (FWHM of a few hundred to a few thousand wave numbers) after complete processing, and the latter are characterized by their negligible or even negative intensities during subsequent processing. We found that, for isolated peaks, the accuracy of this method is very high (frequency determination typically to less than 1 cm^{-1}), but this is not the case for peaks that are closely spaced due to the derivative method that

is used. Deviations from the true peak centers thus depend on the spacing, relative intensities, and line shapes of the individual peaks.

Although Eq. (8) supplies a rather accurate estimate of the number of spectral peaks and the frequencies at which they occur, the information regarding intensities and line shapes is usually not accurate and varies depending on the specific algorithm that is used and the size of the autocorrelation matrix, $\hat{R}$. In order to determine intensities more accurately, we note that most of the inelastic peaks have a FWHM smaller than that of the instrument response function. Hence, they can be reasonably treated as δ functions at this level of approximation. Consequently, Eq. (2) may be rewritten as

$$c(E) \approx \delta(E) + \sum_{k=1}^{M} h_k \delta(E - E_k) , \tag{9}$$

where h_k denotes the integral intensity of the kth vibrational mode, normalized to that of the elastic peak. We next define an error function in the energy domain as follows:

$$\chi_E^2(\mathbf{h}) \equiv \sum_E \left\{ s(E) - i(E) - \sum_{k=1}^{M} h_k i(E - E_k) \right\}^2 , \tag{10}$$

where $\mathbf{h} \equiv (h_1, h_2, \ldots, h_M)^T$. The solution of the equation

$$\nabla_{\mathbf{h}} \chi_E^2(\mathbf{h}) = \mathbf{0} \tag{11}$$

provides an approximate determination of the intensities of the inelastic peaks. The accuracy is dependent on the validity of the δ-function approximation of Eq. (9).

The only remaining issue to be addressed concerns the line shapes of the inelastic peaks, coupled with a refinement of the peak intensities and positions. With this goal in mind, we note that the intrinsic vibrational line shape may be modeled as a Lorentzian function broadened by a Gaussian function (due to a variety of fluctuations normally present in a real system). Consequently, we can construct a system model as follows [cf. Eq. (9)]:

$$C_{\text{model}}(\tau, \mathbf{p}) = 1 + \sum_{k=1}^{M} h_k e^{-iE_k \tau} B_k(\tau) , \tag{12}$$

where

$$B_k(\tau) = \exp\left[-w_{L,k} |\tau| - \left(\frac{w_{G,k}}{2} \tau \right)^2 \right] ,$$

and

$$\mathbf{p} = (h_1, E_1, w_{L,1}, w_{G,1}, \ldots, h_M, E_M, w_{L,M}, w_{G,M})^T .$$

Here, $w_{L,k}$ is the Lorentzian width, and $w_{G,k}$ is the Gaus-

sian width. Next we define an error function in the Fourier domain as follows:

$$\chi_F^2(\mathbf{p}) \equiv \sum_{|\tau| \leq \tau_{max}} |S(\tau) - I(\tau)C_{model}(\tau, \mathbf{p})|^2 \ ; \quad (13)$$

and solving

$$\nabla_{\mathbf{p}}\chi_F^2(\mathbf{p})|_{\mathbf{p}=\mathbf{p_0}} = \mathbf{0} \quad (14)$$

provides the energies of the inelastic peaks, their intensities, and their line shapes [20]. The system transfer function $c(E)$ may be obtained by evaluating the inverse Fourier transform, i.e.,

$$C_{model}(\tau, \mathbf{p_0}) \rightarrow c(E) \ . \quad (15)$$

To demonstrate the power of our methodology, we have applied it to a nearly saturated chemisorbed overlayer of CO on Ru(001), corresponding to a 6 L (1 L = 10^{-6} Torr s) exposure at room temperature, a system that has been well studied by low-energy electron diffraction (LEED) [21], vibrational EELS [22], and IRAS [23]. We have collected new vibrational EELS data for this system with a modest resolution (FWHM of the elastically scattered peak) of 6.7 meV $\cong$ 54 cm^{-1}, and the results are presented in Fig. 1(a) in which 4096 data points were collected with a channel resolution of 2 cm^{-1} and a total collection time of 1000 s. A full description of the EEL spectrometer and the data acquisition scheme is presented elsewhere [2,15,24]. The system transfer function $c(E)$, calculated from Eq. (8) using Marple's algorithm [19], is shown in Fig. 1(b); and the final EEL spectrum after complete processing is shown in Fig. 1(c). There are three different CO stretching modes between 1900 and 2100 cm^{-1}, and five frustrated translations and rotations
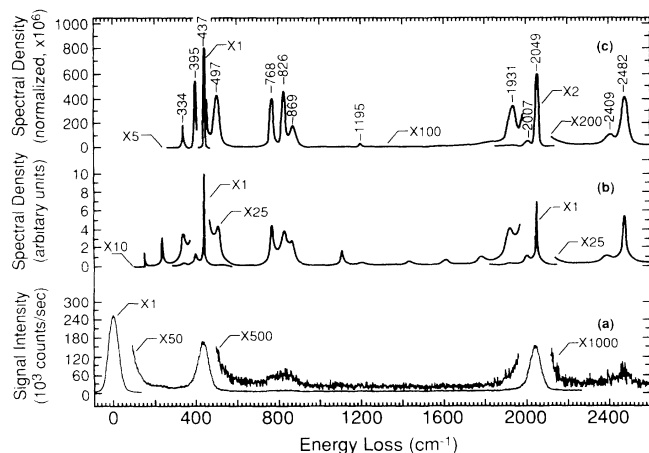

FIG. 1. (a) Measured HREEL spectrum in the specular direction of a saturation coverage of CO on Ru(001) at 300 K. (b) The approximate response function of the CO overlayer given by Eq. (8). (c) The HREEL spectrum after complete processing.

below 500 cm^{-1} [including one at 226 cm^{-1} which is not shown in Fig. 1(c)]. Harmonic and combination bands are apparent between 700 and 900 cm^{-1}, and between 2400 and 2500 cm^{-1}. The three CO stretching modes have a FWHM of 17 cm^{-1} (for the 2049-cm^{-1} peak), 29 cm^{-1} (for the 2007-cm^{-1} peak), and 43 cm^{-1} (for the 1931-cm^{-1} peak); whereas the correlated frustrated translations at 437, 395, and 334 cm^{-1} have FWHM's of 8, 10, and 9 cm^{-1}, respectively. Although a full discussion of these data will be presented elsewhere [15], there are two points to be noted here. First, using IRAS, Pfnür et al. [23] observed a single band centered at 2048 cm^{-1} with a FWHM of 12 cm^{-1} for a saturation coverage of CO on Ru(001) at 300 K [cf. 2049 and 17 cm^{-1} in Fig. 1(c)]. Their slightly more narrow peak and the absence of a small band at 2007 cm^{-1} suggest their overlayer was somewhat better ordered than ours [25]. (Their sensitivity would have precluded their observing the band at 1931 cm^{-1}, even if it had been present.) Furthermore, if we *assume* that the integrated spectral density is proportional to the concentration of the three different kinds of adsorbed CO, we find that 84% of the CO is associated with the 2049-cm^{-1} peak, 13% with the 2007-cm^{-1} peak, and 3% with the 1931-cm^{-1} peak. The accuracy of our frequency determinations is substantiated by the following: (1) The frequency of the dominant CO stretching mode agrees with IRAS data to 1 cm^{-1}; (2) our peaks on both the energy-gain and energy-loss side of the elastic peak agree within 2 cm^{-1}; and (3) the variation in frequency among numerous different measured spectra (for ostensibly the same CO overlayer) is less than 3 cm^{-1}. The sensitivity of the method should be clear by comparing Figs. 1(a) and 1(c). In this connection we might also note that the CO stretching mode at 2049 cm^{-1} on the *energy-gain* side of the elastic peak was clearly observed in the processed spectra even though its average count rate was less than 1 count/s.

Several final comments are appropriate concerning our data processing procedure. First, since by definition $i(E)$ includes various properties of the surface, it must be determined from each measured spectrum. Second, the amplitude of the elastic peak is irrelevant so long as $i(E)$ can be measured accurately and the detector is not operated under saturation conditions. Most important, the success of the method (resolution, sensitivity, and reliability of line-shape determination) is a strong function of the range of data in the Fourier domain [cf. Eq. (6)]. An accurate line-shape determination presents the greatest challenge to the method; having a sufficiently narrow elastic peak and a measured spectrum with a sufficiently high SNR ensures the success of even this difficult endeavor.

To summarize, a data processing methodology has been described that renders vibrational EELS an ultrahigh-resolution spectroscopy. Accurate peak positions, peak intensities, and line-shape functions may be

extracted from measured EELS data. Our methodology should revolutionize both vibrational and electronic EELS measurements, and generalizations of it should find broad applications in other spectroscopic techniques.

[1] F. M. Propst and T. C. Piper, J. Vac. Sci. Technol. **4**, 53 (1967).

[2] W. H. Weinberg, in *Solid State Physics: Surfaces*, edited by R. L. Park and M. G. Lagally, Methods of Experimental Physics Vol. 22 (Academic, Orlando, 1985), p. 23.

[3] H. Ibach and D. L. Mills, *Electron Energy Loss Spectroscopy and Surface Vibrations* (Academic, New York, 1982).

[4] F. M. Hoffmann, Surf. Sci. Rep. **3**, 107 (1983).

[5] Y. J. Chabal, Surf. Sci. Rep. **8**, 211 (1988).

[6] H. Ibach, *Electron Energy Loss Spectrometers: The Technology of High Performance*, Springer Series in Optical Sciences Vol. 63 (Springer-Verlag, Berlin, 1991).

[7] G. Kisters, J. G. Chen, S. Lehwald, and H. Ibach, Surf. Sci. **245**, 65 (1991).

[8] P. A. Cox, W. R. Flavell, A. A. Williams, and R. G. Egdell, Surf. Sci. **152/153**, 784 (1985).

[9] W. T. Petrie and J. M. Vohs, Surf. Sci. **245**, 315 (1991).

[10] G. K. Wertheim, J. Electron Spectrosc. Relat. Phenom. **6**, 239 (1975).

[11] A. F. Carley and R. W. Joyner, J. Electron Spectrosc. Relat. Phenom. **16**, 1 (1979).

[12] B. Voigtländer, D. Bruchmann, S. Lehwald, and H. Ibach, Surf. Sci. **225**, 151 (1990).

[13] C. Astaldi, A. Bianco, S. Modesti, and E. Tossatti, Phys. Rev. Lett. **68**, 90 (1992).

[14] W. F. Maddams, Appl. Spectrosc. **34**, 245 (1980).

[15] Youqi Wang and W. H. Weinberg (to be published).

[16] The instrument response function is defined here as the convolution product of the kinetic energy profile of the incident electron beam, the response function of the electron energy analyzer and detector, and a surface-related function describing broadening due to surface roughness, for example. A constant is also included to account for surface reflectivity, normalization, and units conversion. A detailed derivation is presented elsewhere [15].

[17] J. P. Burg, in *Proc. 37th Meeting Soc. Exploration Geophysicists* (1967); J. P. Burg, Ph.D. dissertation, Stanford University, 1975 (unpublished).

[18] J. N. Kapur, *Maximum-Entropy Models in Science and Engineering* (Wiley, New York, 1989), and references therein; *Modern Spectrum Analysis*, edited by D. G. Childers (IEEE, New York, 1978).

[19] L. Marple, IEEE Trans. Acoustics, Speech, and Signal Process. **28**, 441 (1980).

[20] The nonlinear optimization procedure of Eq. (14) requires a good starting point to ensure reliable results and rapid convergence. This is accomplished by using the results from both the MEM and the linear optimization procedure [cf. Eqs. (8) and (11), respectively].

[21] E. D. Williams and W. H. Weinberg, J. Chem. Phys. **68**, 4688 (1978); Surf. Sci. **82**, 93 (1979).

[22] G. E. Thomas and W. H. Weinberg, J. Chem. Phys. **70**, 1437 (1979).

[23] H. Pfnür, D. Menzel, F. M. Hoffmann, A. Ortega, and A. M. Bradshaw, Surf. Sci. **93**, 431 (1980).

[24] G. E. Thomas and W. H. Weinberg, Rev. Sci. Instrum. **50**, 497 (1979).

[25] This is supported by the following two observations: (1) The CO stretching peaks of Fig. 1(c) are dominated by Gaussian (inhomogeneous broadening) functions; and (2) peaks are present that are characteristic of *very small* amounts of hydrogen and hydrocarbon contamination (at 1105, 1195, and 2966 cm^{-1}).